A hybrid method for Computational Aeroacoustic applied to internal flows

M. Piellard[1], C. Bailly[2]

[1] *Delphi Thermal, Luxembourg, Email: melanie.piellard@delphi.com*

[2] *LMFA – UMR CNRS 5509, Ecole Centrale de Lyon & IUF, France, Email: christophe.bailly@ec-lyon.fr*

Introduction

In an industrial context, the development of an efficient hybrid noise computation method has to consider its applicability and the computing time necessary to reach a relevant solution. In this work, the focus is put on the interpolation of source terms from the CFD mesh to the acoustic mesh, and consequently on the acoustic computation. Indeed, depending on the type of interpolation chosen, the resolution of the acoustic mesh in source regions will have to be close or not to the CFD resolution, which will have a great impact on the computing time and resources necessary for the acoustic finite element simulation.

After introducing the simulation method with theoretical developments, its practical implementation is explained, and the interpolation issue is discussed. The method is then applied to the case of a ducted diaphragm with a low Mach number flow. Finally, conclusions are drawn regarding the interpolation issue.

Simulation method

The simulation method is a two step hybrid approach relying on Lighthill's acoustic analogy [1], assuming the decoupling of noise generation and propagation. The first step consists of an incompressible Large Eddy Simulation of the turbulent flow field, during which a source term is transiently recorded. In the second step, a variational formulation of Lighthill's Acoustic Analogy discretized by a finite element discretization is solved in the Fourier space, leading to the radiated noise up to the free field thanks to the use of infinite elements [2].

Theory

The implementation of Lighthill's acoustic analogy was firstly derived by Oberai *et al* [3], refer also to Actran User's Guide [2] and Caro *et al* [4] for instance. The starting point is Lighthill's equation:

$$\frac{\partial^2}{\partial t^2}(\rho-\rho_0) - c_0^2 \frac{\partial^2}{\partial x_i \partial x_i}(\rho-\rho_0) = \frac{\partial^2 T_{ij}}{\partial x_i \partial x_j} \qquad (1)$$

with

$$T_{ij} = \rho u_i u_j + \delta_{ij}\big((p-p_0) - c_0^2(\rho-\rho_0)\big) - \tau_{ij} \qquad (2)$$

where ρ is the density and ρ_0 its reference value in a medium at rest, c_0 is the reference sound velocity, T_{ij} is Lighthill's tensor, u_i are the velocity components, p is the pressure and τ_{ij} is the viscous stress tensor.

The variational formulation of Lighthill's analogy is then obtained after writing the strong variational statement associated with equation (1), and after integrating by parts along spatial derivatives following Green's theorem. This formulation is actually an equation on the acoustic density fluctuations $\rho_a = \rho - \rho_0$, which reads:

$$\int_\Omega \left(\frac{\partial^2 \rho_a}{\partial t^2}\,\delta\rho + c_0^2 \frac{\partial \rho_a}{\partial x_i}\frac{\partial \delta\rho}{\partial x_i} \right) d\mathbf{x} = -\int_\Omega \frac{\partial T_{ij}}{\partial x_j}\frac{\partial \delta\rho}{\partial x_i}\, d\mathbf{x} + \int_{\partial\Omega=\Gamma} \frac{\partial \Sigma_{ij}}{\partial x_j}\, n_i\, \delta\rho\, d\Gamma(\mathbf{x}) \qquad (3)$$

where $\delta\rho$ is a test function, Ω designates the computational domain, and Σ_{ij} is defined as

$$\Sigma_{ij} = \rho u_i u_j + (p-p_0)\delta_{ij} - \tau_{ij}\,. \qquad (4)$$

Two source terms can be distinguished: a volume and a surface contribution. However, when surfaces are fixed, the latest vanishes. Therefore, only the volume source term is considered in this study.

Practical application of the method

The method consists of coupling a CFD code with a finite element acoustic software where the variational formulation of Lighthill's acoustic analogy is implemented. The main steps of a practical computation, provided that an unsteady solution of the flow field has already been obtained, are as follows:

1. an analysis of the flow field allows to determine in which region(s) of the flow acoustic source terms will be considered; an acoustic mesh is built on the whole region of interest for acoustics, with possibly finer elements in source terms regions;
2. the time history of the source terms, or of useful quantities to compute it, is stored on the CFD mesh during the CFD computation within Fluent 6.3.26 [5];
3. the source terms, computed on the CFD mesh for better accuracy, are interpolated on the usually coarser acoustic mesh;
4. the unsteady source terms are transformed from time to spectral domain;
5. the acoustic computation is performed with Actran/LA [2], taking into account the spectral volume source terms.

On the interpolation

In these five steps, the third one, namely the interpolation from the CFD mesh to the acoustic mesh, is of primary importance. Indeed, all the interest of this hybrid aeroacoustic method resides in the decoupling of the noise generation from its propagation. The decoupling makes it possible to adapt each computational step with respect to its efficiency. In particular, the requirements in terms of grid resolution are usually one order of magnitude more severe in the CFD than in the acoustic computation. This is due to the difference in size of acoustic and turbulent wavelengths. Therefore, in order to keep a light and tractable acoustic mesh, an efficient interpolation of source terms from the CFD mesh to the acoustic mesh has to be defined.

In this work, two types of interpolation are applied. A classical 4th order Lagrange polynomial interpolation is compared to a conservative interpolation, in which an integration of source terms on the acoustic finite elements is performed.

The ducted diaphragm at low Mach number

Presentation

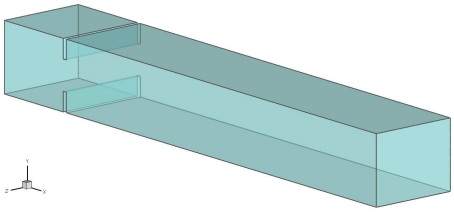

Figure 1: Diaphragm geometry. The x-axis indicates the streamwise flow direction; y- and z-axis respectively indicate the transverse and spanwise directions.

The case of the ducted diaphragm at low Mach number has been described extensively in Piellard *et al* [6, 7]. It consists of a duct of rectangular cross-section obstructed by a diaphragm of height h, see Figure 1. This geometry is of particular interest since it represents an internal low velocity flow, for which few computational aeroacoustic studies are available.

Numerical study on a slice of the domain

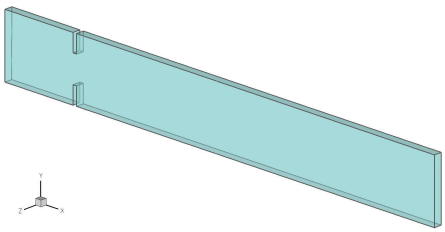

Figure 2: Diaphragm slice geometry.

A first study is performed on a slice of the domain consisting of 10% of the real width; a sketch of this reduced domain is given in Figure 2. An incompressible Large Eddy Simulation is carried out on a refined mesh of this domain, where the finest cells in the area of the diaphragm and downstream of the diaphragm are of the order $h/70$. Aerodynamic results are favorably compared [7] to the LES simulation of Gloerfelt & Lafon [8], despite the truncation in the third direction. The main effect of the domain truncation is to constrain the flow to an exagerated two-dimensional behavior.

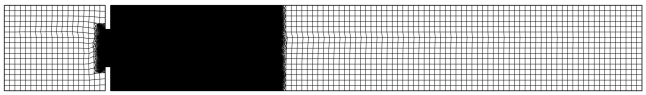

Figure 3: Diaphragm slice acoustic mesh.

An acoustic computation is performed in the central XY plane of the CFD domain. The acoustic mesh is identical to the CFD mesh in the first part of the outlet duct and in the diaphragm region, and coarser elsewhere. The largest elements reach the mesh size of $h/7$, see Figure 3, allowing to propagate the acoustic waves up to 10,000 Hz. As the acoustic mesh is identical to the CFD mesh where source terms are computed, no interpolation is required to input the source terms in the acoustic computation. Source terms are defined only in the region of mesh refinement. Spatial filtering is also applied at the end of the source region to ensure a smooth transition to zero of the source terms toward the domain exit, see [6] for details.

Numerical study on the 3D domain

In this second study, an incompressible Large Eddy Simulation is performed on the complete three-dimensional domain, on a mesh very similar to the previous one, with the finest cells downstream of the diaphragm of the order $h/70$. For this simulation, almost no difference is noticed with reference [8] regarding aerodynamic results, and the complex three-dimensional behavior of the flow is described in [6].

Figure 4: Diaphragm refined acoustic mesh.

Two acoustic meshes are built. The first one is extremely refined in the first part of the outlet duct, with the cell size equal to twice the CFD mesh size, see Figure 4. Because the acoustic mesh is not identical to the CFD mesh in source regions, interpolation is required to define acoustic source terms on the acoustic mesh. A classical, non conservative 4th order Lagrange polynomial interpolation is performed. Source terms are defined only in the region of mesh refinement.

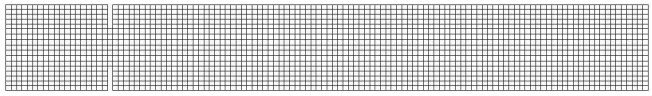

Figure 5: Diaphragm coarse acoustic mesh.

The second acoustic mesh is built only with acoustic

wave propagation requirements, without considering the presence or not of source terms. The mesh is uniform with a cell size of $h/7$ in the whole domain, see Figure 5. In this case where interpolation is once more required, a new conservative interpolation scheme developed by Free Field Technologies [9] is applied. This interpolation actually consists in integrating source terms over the acoustic finite elements, preserving the energy contained in the source terms. For the corresponding acoustic computation, source terms are defined in the whole domain. Spatial filtering is also applied in the second part of the outlet duct to ensure a smooth transition to zero of the source terms toward the domain exit.

Acoustic results

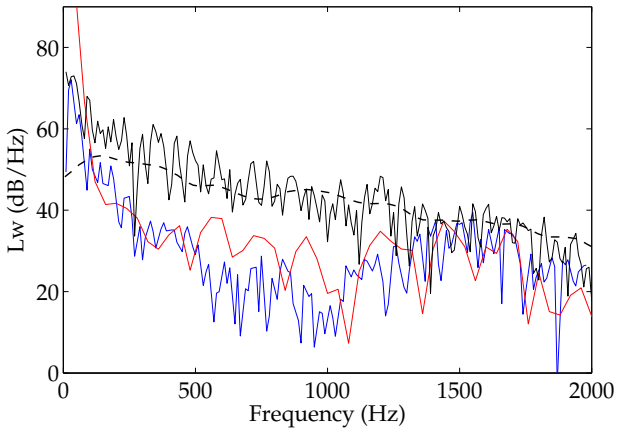

Figure 6: Acoustic results: acoustic power radiated at the end of the outlet duct. – – –: reference results of Gloerfelt & Lafon [8]. ——: 2D computation without interpolation, with spatial filtering. ——: 3D computation with Lagrange interpolation. ——: 3D computation with conservative interpolation, i.e. integration, with spatial filtering.

Acoustic results are given in terms of acoustic power radiated at the end of the outlet duct in Figure 6. It appears that, in spite of the limitations of the CFD slice computation, the corresponding two-dimensional acoustic simulation, without interpolation, gives good results, with in particular the spectrum broadband shape similar to reference [8], over the whole frequency range [0–2000] Hz.

By contrast, three-dimensional results on the finest acoustic mesh, with Lagrange polynomials interpolation, presents a broadband spectrum shape very different from the reference; a loss of energy in the frequency range [100–1400] Hz is particularly visible. This loss of energy is attributed to the information loss during interpolation, where roughly only 1/8th of the source terms information was kept, which corresponds to a decimation by 2 in each space direction from the CFD to the acoustic mesh.

Slightly better results are obtained with the coarse three-dimensional acoustic mesh using integrated source terms. Note that in this last computation, only 25 ms of signal was available, while 100 ms were considered in previous simulations. The mandatory signal windowing (Hanning) has thus a great influence, and better results are expected with a longer simulation time.

Conclusion

In this work, the focus is put on the comparison of different strategies of source term interpolation from the CFD mesh to the acoustic mesh. With no surprise, the best acoustic results are obtained when the CFD and the acoustic meshes are identical, requiring no interpolation at all for the source terms; this corresponds to the study on a slice of the domain. When interpolation is required, which is often the case since an acoustic mesh as fine as the CFD mesh is not tractable in most applications, even a high order classical interpolation is not sufficient to provide relevant results; the loss of information during non conservative interpolation cannot be retrieved by increasing the interpolation order. Besides, the use of a conservative interpolation, consisting here of source terms integration, allows a more accurate representation of the source terms while preserving their energy. This last solution gives better results than classical interpolation, and will be further investigated.

Acknowledgments

The first author would like to greatly acknowledge Free Field Technologies for the help and support provided together with their latest developments of Actran/LA.

References

[1] Lighthill, M.J., On sound generated aerodynamically. I: General theory. *Proc. Roy. Soc. London* **A211**, pp. 564-587, 1952.

[2] Free Field Technologies, *Actran 2006 – Aeroacoustic solutions, User's manual*, 2006.

[3] Oberai, A. A., Ronaldkin, F., and Hughes, T. J. R., Computational procedures for determining structural-acoustic response due to hydrodynamic sources, *Comput. Meth. in Applied Mech. and Eng.*, Vol. 190, 2000, pp. 345–361.

[4] Caro, S., Ploumhans, P., and Gallez, X., Implementation of Lighthill's Acoustic Analogy in a finite/infinite elements framework, *AIAA Paper 2004–2891*, 2004.

[5] Fluent Inc., *Fluent 6.3 User's Guide*, Sept. 2007.

[6] Piellard, M. and Bailly, C., Validation of a hybrid CAA method. Application to the case of a ducted diaphragm at low Mach number. *AIAA Paper 2008-2873*, 2008.

[7] Piellard, M., A hybrid method for Computational AeroAcoustics applied to confined geometries. *PhD Thesis*, Ecole Centrale de Lyon, 2008–25.

[8] Gloerfelt, X. and Lafon, P., Direct computation of the noise induced by a turbulent flow through a diaphragm in a duct at low Mach number. *Computers & Fluids* **37**(4), 2008, pp. 388–401.

[9] Free Field Technologies, *Actran 2009 for Aeroacoustic, User's manual*, URL: `www.fft.be`, 2009.